Journal of General Virology (2005), **86**, 1403–1413 DOI 10.1099/vir.0.80427-0

Yellow fever virus NS2B–NS3 protease: characterization of charged-to-alanine mutant and revertant viruses and analysis of polyprotein-cleavage activities

Thomas J. Chambers,[1] Deborah A. Droll,[1] Yujia Tang,[1] Yan Liang,[1] Vannakambadi K. Ganesh,[2] Krishna H. M. Murthy[2] and Michael Nickells[1]

[1]Department of Molecular Microbiology and Immunology, Saint Louis University School of Medicine, 1402 South Grand Avenue, St Louis, MO 63104, USA

[2]Center for Macromolecular Crystallography, University of Alabama at Birmingham, 79-THT, MCLM-244, 1918 University Boulevard, Birmingham, AL 35294-0005, USA

Correspondence
Thomas J. Chambers
thomas_chambers2@merck.com

A series of 46 charged-to-alanine mutations in the yellow fever virus NS2B–NS3 protease, previously characterized in cell-free and transient cellular expression systems, was tested for their effects on virus recovery. Four distinct plaque phenotypes were observed in cell culture: parental plaque-size (13 mutants), reduced plaque-size (17 mutants), small plaque-size (8 mutants) and no plaque-formation (8 mutants). No mutants displayed any temperature sensitivity based on recovery of virus after RNA transfection at 32 versus 37 °C. Most small plaque-mutants were defective in growth efficiency compared with parental virus. However not all small plaque-mutants had defective 2B/3 cleavage, with some showing selective defects at other non-structural protein cleavage sites. Revertant viruses were recovered for six mutations that caused reduced plaque sizes. Same-site and second-site mutations occurred in NS2B, and one second-site mutation occurred in the NS3 protease domain. Some reversion mutations ameliorated defects in cleavage activity and plaque size caused by the original mutation. These data indicate that certain mutations that reduce NS2B–NS3 protease cleavage activity cause growth restriction of yellow fever virus in cell culture. However, for at least two mutations, processing defects other than impaired cleavage activity at the 2B/3 site may account for the mutant phenotype. The existence of reversion mutations primarily in NS2B rather than NS3, suggests that the protease domain is less tolerant of structural perturbation compared with the NS2B protein.

Received 7 July 2004
Accepted 13 January 2005

INTRODUCTION

Yellow fever virus (YFV), the prototype member of the genus *Flavivirus* in the family *Flaviviridae* contains a single-stranded, positive-sense RNA genome of 10 862 nt, encoding a long polyprotein precursor (Lindenbach & Rice, 2001). Production of mature viral proteins occurs by cleavage of the polyprotein in association with membranes of the endoplasmic reticulum (ER). Signal peptidase cleavages generate the structural proteins and the amino terminus of NS4B. An unidentified ER-resident protease mediates cleavage of the NS1–NS2A precursor (Falgout & Markoff, 1995). The remaining cotranslational cleavages, as well as a maturation cleavage of the membrane-anchored capsid protein, are carried out by the NS3 protease in conjunction with its NS2B cofactor (Amberg *et al.*, 1994; Cahour *et al.*, 1992; Chambers *et al.*, 1991; Falgout *et al.*, 1991; Lobigs, 1992, 1993; Preugschat *et al.*, 1990; Preugschat & Strauss, 1991; Wengler *et al.*, 1991; Yamshchikov & Compans, 1994, 1995; Yusof *et al.*, 2000; Zhang *et al.*, 1992). These occur at consensus cleavage sites (anch C/virion C, 2A/2B, 2B/3, 3/4A, 4A/2K and 4B/5), and an alternative cleavage site ($2A^{\alpha}$) (Nestorowicz *et al.*, 1994). An internal cleavage of NS3 has also been described (Arias *et al.*, 1993; Teo & Wright, 1997). The amino-terminal domain of NS3 (residues 1–181 for YF) contains a trypsin-like serine protease domain (Bazan & Fletterick, 1989; Gorbalenya *et al.*, 1989) that exhibits preference for cleavage sites containing two basic amino acids, KR or RR, or in some cases QR or QK, (Lin *et al.*, 1993a, b; Nestorowicz *et al.*, 1994), within the consensus sequence G/ARR−S/G (Chambers *et al.*, 1995). Solution of the crystal structure of the NS3 protease of dengue-2 virus confirms the features typical of the trypsin family of serine proteases (Murthy *et al.*, 1999).

In previous studies, it was established that NS3 cleavage activity is necessary for correct processing of the viral polyprotein and for virus replication (Chambers *et al.*, 1990b;

Wengler *et al.*, 1991). NS3 and NS2B form a stable complex that cleaves the polyprotein substrate in *cis* and in *trans* (Arias *et al.*, 1993; Chambers *et al.*, 1993; Falgout *et al.*, 1993), although the factors governing the sequence of cleavages needed for assembly of RNA replication complexes remain poorly understood. The molecular basis for NS2B–NS3 complex formation involves both a conserved central region within NS2B, and the amino-terminal region of NS3 (Chambers *et al.*, 1993; Droll *et al.*, 2000; Falgout *et al.*, 1993). Within the conserved region, there is a potential peptide cofactor analogous to that of the NS4A protein that complexes with the NS3 protease of hepatitis C virus (Brinkworth *et al.*, 1999; Butkiewicz *et al.*, 1996; Lin *et al.*, 1995). However, for YFV, charged amino acids are involved in the complex formation. In previous studies, we analysed a series of charged-to-alanine mutations within the NS2B–$NS3_{181}$ polyprotein for effects on processing of the viral polyprotein (Droll *et al.*, 2000). Because these mutations caused a range of effects on cleavage efficiency, it was of interest to determine what effects impairment of cleavage activity would have on viral infectivity. Identification of mutations that are deleterious for virus replication but do not interfere with cleavage activity could suggest novel functions of either NS2B or NS3 based on protein–protein interactions with other viral or host proteins.

METHODS

Cells and viruses. SW-13 cells (human adrenocortical carcinoma cells), BHK-21, and C6/36 cells were originally obtained from the ATCC and were grown in alpha minimal essential media (MEM) plus 10 % fetal bovine serum (FBS). SW-13 cells were grown at 37 and 32 °C. C6/36 cells were grown at 30 °C. Plaque assay for virus titration was done on SW-13 cells overlaid with 1 % agarose (Seakem ME; FMC Bioproducts) and 5 % FBS, incubated at 37 °C. Plaques were visualized between 4 and 7 days post-infection, by staining with crystal violet.

Plasmid constructions. Mutations were originally created in pET/BS-NS2B–$NS3_{181}$ as described previously using a QuikChange Site-Directed Mutagenesis protocol (Stratagene) (Droll *et al.*, 2000). pET/BS-NS2B–$NS3_{181}$ (formerly named pET/BS-NS2B–3·1) is a phagemid, derived originally by engineering an *Fsp*I/*Sca*I restriction fragment from pBluescriptII SK(+) (Stratagene) containing the f1 origin, into pET8C-NS2B–3·1, as described previously (Chambers *et al.*, 1990b). The transcription vector pET8C (Studier *et al.*, 1990) contains a promoter for T7 RNA polymerase, followed by a unique *Nco*I site with an ATG in an appropriate context for eukaryotic expression. pET8C-NS2B–3·1 was originally created by inserting a PCR-amplified fragment obtained from YFM5·2 DNA (Rice *et al.*, 1989), encompassing the NS2B–$NS3_{181}$ region together with a 5′ *Nco*I site and a 3′ *Bam*HI site adjacent to a translation termination codon, into pET8C using *Nco*I and *Bgl*II restriction sites, as described (Chambers *et al.*, 1990b).

For transient expression experiments of mutant YF non-structural polyproteins in SW-13 and BHK-21 cells, mutations in pET/BS-NS2B–$NS3_{181}$ were subcloned into pET/BS-sig2A–5_{356} (Chambers *et al.*, 1991). *Sac*I and *Pvu*II restriction sites were used to introduce the mutations from pET/BS-NS2B–$NS3_{181}$ into pET/BS-sig2A–5_{356}. YF5·2iv templates needed for the generation of infectious YF RNA transcripts containing the mutations required engineering the individual NS2B or NS3 mutations into pYFM5·2, which is part of a two-plasmid system used for production of *in vitro*-ligated full-length viral transcription templates (Rice *et al.*, 1989), as described below. The mutations were exchanged from pET/BS-sig2A–5_{356} into pYFM5·2 using *Avr*II and *Ngo*MI restriction sites. Presence of the desired mutations in pYFM5·2 was confirmed by nucleotide sequencing.

Cell-free translation. Protease cleavage activity at the 2B/3 cleavage site was analysed by cell-free translation by using the TNT Coupled Reticulocyte Lysate system (Promega). Reactions were run as recommended by the manufacturer except reaction volumes were scaled down to half the volume (25 instead of 50 µl). Reactions were programmed with 1 µg unlinearized plasmid DNA (parental pET/BS-NS2B–$NS3_{181}$ or various mutant derivatives). Translation products were labelled by the addition of 1 µCi (37 kBq) of [^{35}S]methionine (0·4 mCi µl^{-1}) per reaction, and run for 20, 45 and 90 min. For reactions run in the presence of canine pancreatic microsomal membranes (Y4041; Promega), 1·5 µl stock membrane preparation was added to each reaction, which in control experiments was sufficient to glycosylate the control protein and to cleave the signal sequence from the control protein. Translation products were immunoprecipitated by using conditions previously described (Droll *et al.*, 2000), and analysed on SDS-PAGE with imaging by fluorography.

Transient expression of sig2A–5_{356} polyproteins. Transfection of the pET/BS-sig2A–5_{356} plasmid for expression of the YF non-structural polyprotein containing the 2A/2B, 2B/3, 3/4A, 4A/2K, 2K/4B and 4B/5 cleavage sites was done in SW-13 and BHK-21 cells essentially as described previously (Droll *et al.*, 2000), except for the use of lipofectamine. Cells were preinfected with vaccinia virus vTF7-3 (10 p.f.u. per cell), which encodes the bacteriophage T7 RNA polymerase under the control of an early vaccinia promoter, and then transfected with plasmid DNA to drive RNA synthesis from the T7 promoter encoded upstream of the YF non-structural protein genes. Transfection reactions were done in six-well costars by the addition of a mixture of 4 µl Lipofectamine, 6 µl Plus reagent (Invitrogen) and 1 µg caesium-banded plasmid DNA in a final volume of 400 µl α-MEM per well. Transfection was continued for 2·5 h, followed by addition of [^{35}S]methionine and labelling for an interval of 4·5–5 h. Cells were harvested by the addition of 0·5 ml SDS lysis buffer (0·5 % SDS, 10 mM Tris/HCl pH 7·5, 150 mM NaCl, 1 mM EDTA) at 25 °C, sheared by passage through a 26-gauge needle and centrifuged in an Eppendorf centrifuge for 10 min to remove insoluble material. SDS lysates were diluted to 1 × Triton solution (1 % Triton X-100, 10 mM Tris/HCl pH 7·5, 150 mM NaCl, 1 mg BSA ml^{-1}), and chilled at 4 °C for 15 min. Virus-specific proteins were immunoprecipitated with specific rabbit polyclonal antisera to the YF NS2B, NS3 or NS4B proteins as described previously (Chambers *et al.*, 1990a) and immunoprecipitates were analysed by SDS-PAGE on 10–13 % SDS gels as previously described (Chambers *et al.*, 1990a; Droll *et al.*, 2000).

Transcription and transfection. A two-plasmid system for construction of YF5·2iv virus templates was used as previously described (Rice *et al.*, 1989). The templates were assembled by ligation of the appropriate restriction fragments, and full-length RNA transcripts were synthesized by using SP6 RNA polymerase in the presence of 5′ cap analogue (New England Biolabs). Transfections were done by incubating Vero cells at 25 °C for 10 min in the presence of a mixture of 100–300 ng RNA transcripts and 20 µl lipofectin (Gibco-BRL) in PBS in a reaction volume of 500 µl. Transfected cell cultures were incubated at either 32 or 37 °C and viruses were harvested at the time of onset of cytopathic effects, usually at 5 to 7 days after transfection. Virus yields were determined by plaque assay on SW-13 cells and plaque sizes were determined as the mean diameters of 10 well-isolated plaques.

Plaque purification. Mutant viruses recovered from RNA transfections were plaque-purified three times in SW-13 cells with

amplification on BHK-21 cells. Concentrated virus stocks were prepared for some of the mutants by precipitation with PEG-8000. The virus solution was adjusted to a concentration of 10 % PEG-8000 in TNE (120 mM NaCl, 12 mM Tris/HCl pH 8·0, 1 mM EDTA), the material was placed on ice for 1 h, and the precipitated virus was recovered by centrifugation in a Sorvall centrifuge using a GSA rotor at 5000 r.p.m. for 30 min at 4 °C. The pellet was gently washed twice with TNE, and finally resuspended in alpha-MEM plus 20 % fetal calf serum, at 1 : 100 of the original volume of the virus solution. Virus was aliquotted and stored at −70 °C until use.

Growth curve analysis. Growth curve experiments were done by infecting SW-13 or C6/36 cell monolayers at an m.o.i. ranging from 1 to 5 (m.o.i. of 5 were used unless limited by titre of the virus). Parental and mutant growth curve infections were always in parallel using identical m.o.i values. Media were harvested at approximately 12–24 h intervals and replaced with fresh media (alpha-MEM plus 3 % FBS). Samples were assayed in triplicate by plaque assay on SW-13 cells.

Isolation and sequencing of revertant viruses. Plaque-revertant viruses were isolated during plaque purification of the mutant viruses, and subjected to at least one round of plaque purification in duplicate for each revertant undergoing characterization. RNA was prepared from the plaque isolates by extraction of infected cell monolayers with Trizol (Gibco-BRL). One microgram of RNA was reverse-transcribed using Superscript II (Gibco-BRL), in the presence of an antisense oligonucleotide primer corresponding to YF nt 5300–5320. cDNA was amplified by PCR using the same 3′ primer and a 5′ primer (nt 4141–4160), encompassing the NS2B–$NS3_{181}$ region, in the presence of *Taq* DNA polymerase (Gibco-BRL). PCR products were purified with Wizard PCR preps kits (Promega), and sequenced using BigDye chain terminator reactions on a Becton Dickinson ABI DNA sequencer.

Construction of plasmids containing reversion mutations. Mutations identified by sequencing of PCR products from plaque-purified revertant viruses were subcloned directly into pET/BS-NS2B–$NS3_{181}$ using available restriction sites. Where this was not possible, PCR products were reamplified using the 3′ primer YF 5300, and a 5′ primer incorporating an *Xba*I site adjacent to the 5′ terminus of the NS2B region, and cloning the resulting PCR product into pET/BS-NS2B–$NS3_{181}$ using the *Xba*I and *Hpa*I restriction sites. In some cases, the PCR products were initially subcloned into the TOPO-TA vector (Invitrogen), before cloning into pET/BS-NS2B–$NS3_{181}$.

Molecular modelling. A homology model for the YFV NS3 protease was derived on the basis of the reported crystal structure of the dengue-2 protease (PDB accession no. 1bef; GenBank accession no. M14969), using the template and coordinates provided by the Swiss-modeller program. Figs were drawn using graphic programs supplied by the modelling server.

RESULTS

Construction of mutant viruses

In a previous study, a series of charged-to-alanine mutations in the NS2B–$NS3_{181}$ region of the YFV polyprotein were found to have variable effects on cleavage activity at the 2B/3 cleavage site in cell-free and cellular expression assays (Droll *et al.*, 2000). In particular, two charge clusters (mutants 2·4, 2·5 at the amino terminus of the conserved domain of NS2B; and mutants 3·6, 3·61, and 3·62, in the amino terminus of NS3) were found to have deleterious effects on 2B/3 cleavage and *trans* association of the NS2B and NS3 proteins. Based on these observations, we then tested for correlations between the level of cleavage activity of a given mutant NS2B–$NS3_{181}$ polyprotein, and the growth and plaque formation of YF viruses containing the corresponding mutations, to determine if protease cleavage activity in the expression assays is related to virus production in infected cells. Although mutants 2·4 and 2·5 yielded small plaque-mutants that were of further interest to study, mutation 3·6 was lethal, and 3·61 and 3·62 yielded viruses with only reduced plaque-size. Unexpectedly however, very small plaques were produced by several mutations that did not impair 2B/3 cleavage (see below).

Fig. 1 illustrates the mutations which were engineered into the YF5·2iv molecular clone. Table 1 summarizes the data on recovery of viruses, their relative plaque sizes formed at 37 °C on SW-13 cells, and the corresponding level of 2B/3 cleavage activity based on cell-free assay (Droll *et al.*, 2000). The mutations had variable effects on recovery of infectious virus and plaque size. Thirteen mutants had a parental phenotype (> 90 % of parental size). Seventeen mutants had a reduced plaque-phenotype (50–90 % of parental size). Eight mutants had a small plaque-phenotype (< 50 % of parental). Eight mutants did not form plaques. Four mutations were not tested for recovery of virus. Virus titres after RNA transfection indicated no severe defect in replication efficiency for those mutants detectable by plaque assay, based on recovery of more than 10^4 p.f.u. virus ml^{-1}. Furthermore, transfection at 32 versus 37 °C yielded no evidence that any mutant displayed a temperature-sensitive phenotype. In these experiments, virus yields from the transfection harvest for the parental YF5·2iv were in the range of 5×10^6 to 1×10^7 p.f.u. ml^{-1}.

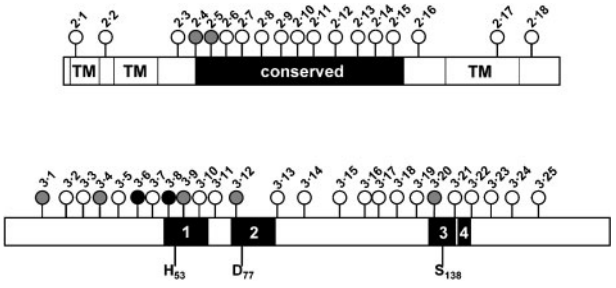

Fig. 1. Schematic of the NS2B–NS3 protease and the charged-to-alanine substitutions tested for effects on virus replication. Mutations involving single or multiple charge cluster substitutions are shown as previously described (Droll *et al.*, 2000). Predicted topologic regions of NS2B are shown (TM indicates putative transmembrane regions). Conserved indicates the conserved central domain of NS2B containing the predicted peptide cofactor for NS3 (Brinkworth *et al.*, 1999). For NS3, homology boxes (1, 2, 3 and 4) (Gorbalenya *et al.*, 1989) and residues of the catalytic triad (H_{53}, D_{77}, S_{138}) are shown. Mutations which caused marked inhibition of 2B/3 cleavage are in black. Grey shading indicates mutations with mild to moderate inhibition of 2B/3 cleavage. White shading indicates minimal or no effect on 2B/3 cleavage. For clarity, mutants 2·41–2·45 and 3·61–3·62 are not shown.

Table 1. Recovery of mutant viruses

+/+ or −/− indicates recovery at 32 or 37 °C, respectively. Parentheses indicate mutants tested in growth curve experiments. NA, Not applicable; NT, not tested.

Virus	Plaque size	Recovery 32/37 °C	2B/3 cleavage*
	Parental		
WT	100	+/+	96–98
2·8	115	+/+	93
2·9	99	+/+	98
2·11	123	+/+	96
2·12	131	+/+	99
2·14	93	+/+	98
2·16	119	+/+	94
2·17	93	+/+	95
3·1	91	+/+	86
3·10	97	+/+	98
3·13	102	+/+	96
3·20	103	+/+	89
3·23	91	+/+	98
3·11	92	+/+	92
	Reduced		
2·6	85	+/+	99
2·7	78	+/+	97
2·13	86	+/+	97
2·15	76	+/+	98
2·41	77	+/+	69
2·42	82	+/+	65
3·2	63	+/+	90
3·3	89	+/+	99
3·5	78	+/+	98
3·61†	63	+/+	70
3·62†	51	+/+	19
3·14	88	+/+	96
3·16	86	+/+	99
3·17	76	+/+	99
3·18	76	+/+	96
3·19	89	+/+	98
3·24	75	+/+	99
	Small		
2·3†‡	<10	+/+	92
2·4†‡	39	+/+	66
(2·5)†‡	39	+/+	80
2·18†‡	22	+/+	95
(3·7)	27	+/+	93
(3·12)	41	+/+	88
(3·15)‡	33	+/+	92
(3·22)	40	+/+	97
	Absent		
2·2	NA	−/−	97
2·10	NA	−/−	95
3·4	NA	−/−	87
3·6	NA	−/−	0·4
3·8	NA	−/−	6
3·9	NA	−/−	88
3·21	NA	−/−	97
3·25	NA	−/−	98
	Not tested		
2·1	NT	NA	97
2·43	NT	NA	24
2·44	NT	NA	19
2·45	NT	NA	5

*Data from Droll *et al.* (2000).
†Mutants for which plaque revertants were isolated.
‡Mutants tested in cell-free and cellular cleavage assays.

Mutant viruses selected for further study by growth curve analysis, polyprotein cleavage assays and revertant characterization are indicated in the table.

In general, there was not a uniform correlation between 2B/3 cleavage efficiency and plaque phenotype. Twelve of 13 mutants with parental plaque-size had parental levels of cleavage activity. However, 22 mutants exhibited parental levels of 2B/3 cleavage activity (>90 % of parental) but were deleterious (18 of 22) or lethal (4 of 22) for plaque formation. Decreased cleavage activity (<90 % of parental) was associated with reduced or small plaque-size in seven cases, and no recovery of virus in four cases. Mutant 3·20 was an exception, since it had reduced cleavage activity but a parental plaque-size.

Growth curve analysis

To determine if reduced plaque-size reflected impaired replication efficiency as measured by virus production in cell culture, a number of the small plaque-mutant viruses were selected for growth curve analysis. Mutants that exhibited a range of cleavage efficiency at the 2B/3 cleavage site were studied (2·5, 3·7, 3·12 and 3·22). However, not all mutants could be studied in this way because either a high rate of plaque reversion precluded preparation of some plaque-purified virus stocks (2·3 and 2·18) or execution of the growth curve was complicated by appearance of plaque revertants (2·4). Results of the growth curve studies are shown in Fig. 2(a)–(d). Studies were done in SW-13 cells at 37 and 32 °C to screen for temperature sensitivity, and for some mutants also in C6/36 cells at 30 °C, to extend the range for temperature-sensitive screening, and test for any evidence of host-restriction of virus replication.

Fig. 2(a) shows results for mutant 2·5, which caused a moderate decrease in cleavage at the 2B/3 site (80 % of parental), and caused a plaque size of 39 %. Mutant 2·5 exhibited a decrease in the rate of virus accumulation and a lower peak of virus production at 37 °C (panel i) compared with the parental virus (approx. 0·75 log p.f.u. ml^{-1}). At 32 °C (panel ii), the rate of virus production was initially comparable to the parental virus, but the peak titre was approximately 0·75 log p.f.u. ml^{-1} less.

Fig. 2(b) shows results for mutation 3·12, which caused

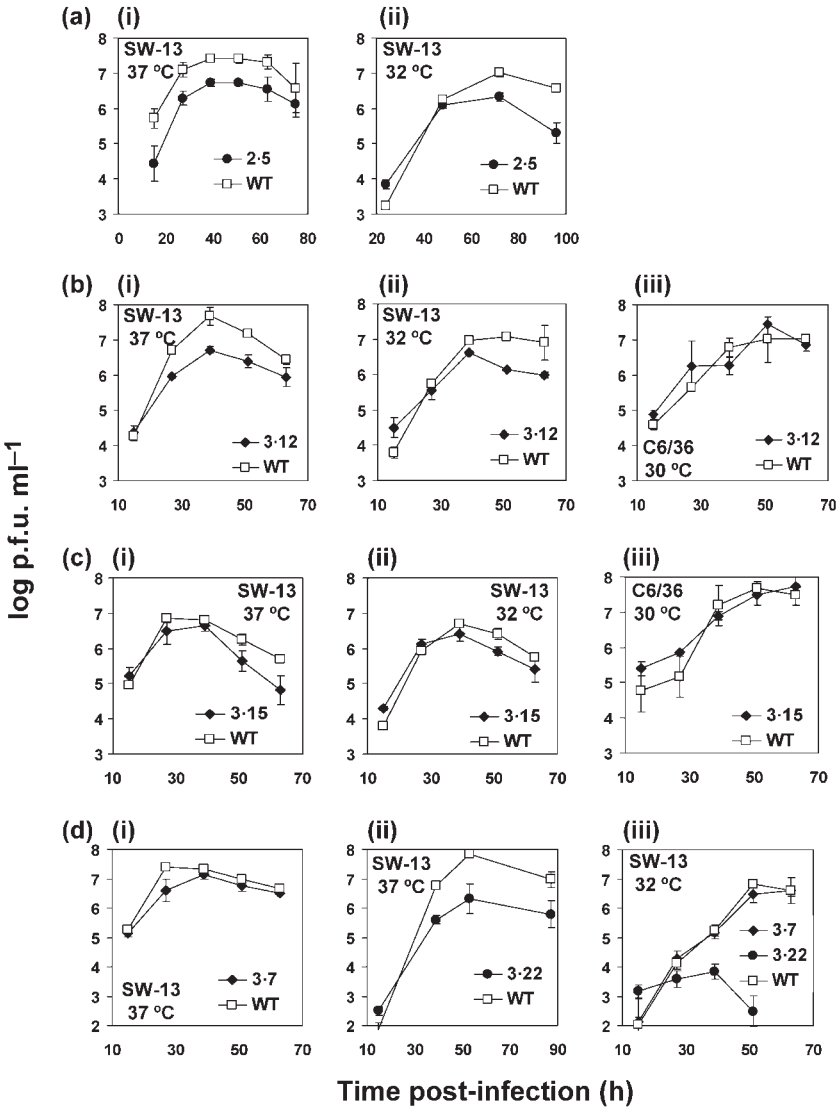

Fig. 2. Growth curves of mutant viruses. Experiments were performed as described in Methods. Virus yields are indicated as mean ± standard deviation. (a) Mutant 2·5 at 37 °C and 32 °C in SW-13 cells. (b) Mutant 3·12 at 37 °C, 32 °C in SW-13 cells and at 30 °C in C6/36 cells. (c) Mutant 3·15 at 37 °C, 32 °C in SW-13 cells and at 30 °C in C6/36 cells. (d) Mutant 3·7 at 37 °C, mutant 3·22 at 37 °C and mutants 3·7 and 3·22 at 32 °C in SW-13 cells.

a mild decrease in 2B/3 cleavage (88 %), and caused a small plaque-size (41 % of parental virus). Its growth was characterized by reduced virus production at 37 °C (panel i) (1 log lower peak-titre than the parent virus), but a less severe defect at 32 °C (panel ii) (0·3 log lower peak-titre), in SW-13 cells. Growth in C6/36 cells at 30 °C (panel iii) was similar to parental virus, suggesting increased stability of the mutant virus at this temperature.

Fig. 2(c) shows the results for mutation 3·15, which caused no defect in cleavage at the 2B/3 site (91·7 %), and caused a small plaque-size (33 % of parental size). It exhibited a small reduction in virus production at both 37 and 32 °C (panels i and ii, respectively), with decreases of 0·4 and 0·3 logs of virus, respectively, on SW-13 cells. Growth on C6/36 cells did not reveal a defect in peak virus production (panel iii).

Mutation 3·7 exhibited no defect in 2B/3 cleavage and caused a very small plaque-size (27 % of parent). Fig. 2(d) shows that it was slightly reduced in growth efficiency at 37 °C (panel i) (0·4 log lower peak-titre), and only minimally at 32 °C (panel iii) on SW-13 cells (Fig. 2d). Mutant 3·22 was not impaired in 2B/3 cleavage but caused a small plaque-phenotype (40 % of parent). Fig. 2(d) shows that it exhibited a moderate defect in peak virus production at 37 °C (panel ii) (1·5 log reduction) and a profound defect at 32 °C (panel iii) (3 log reduction).

Taken together, these results show that reduced plaque sizes of the mutant viruses which were examined were usually associated with decreased virus production, although the extent of reductions in virus yields were variable among the mutants. For the mutants 3·12 and 3·15, experiments in C6/36 cells did not reveal any evidence of host-restriction of virus production.

Characterization of revertant mutations

During plaque purification of the mutant viruses, plaque-revertant viruses with increased plaque size compared with the original transfection harvests of the mutant viruses, were observed for mutants 2·3, 2·4, 2·5, 2·18, 3·61 and 3·62. To gain insight into whether novel mutations in the NS2B or NS3 proteins might be involved in the revertant

phenomena, PCR products derived from the NS2B–$NS3_{181}$ region of these revertant viruses were sequenced. This analysis revealed three classes of mutations associated with plaque reversion (Table 2). Same-site mutations involving different amino acids than the parental residue were observed for two of the revertants of mutant 2·3 (2·3·1 had substitution of residue 47 with glutamic acid instead of the parental arginine and 2·3·3 had substitution of residue 49 with serine instead of the parental aspartic acid); and for the revertant of mutant 2·4 (substitution of residue 54 with valine instead of the parental lysine). Same-site mutations involving the parental amino acid residue occurred for revertants of mutants 3·61 and 3·62, (substitution with parental glutamic acid and aspartic acid residues, respectively). Second-site mutations were observed for one revertant of mutant 2·3, (2·3·2 had substitution of serine for alanine at residue 45, adjacent to the original mutations at residues 47 and 49), and for mutant 2·18, (substitution of a histidine for leucine at residue 122, adjacent to the original mutations at residues 124 and 126). Another type of second-site mutation occurred for the revertant of mutant 2·5, involving substitution of tryptophan for arginine at amino acid residue 62 in the NS3 region.

Effects of reversions on NS2B–$NS3_{181}$ cleavage activity

If the second-site mutations were involved in the plaque-reversion process, it is expected that they would exhibit compensatory effects on defects in protease cleavage activity caused by the original engineered mutations. To evaluate this hypothesis, pET/BS-NS2B–$NS3_{181}$ plasmids were engineered for those mutations that yielded plaque-reversion mutations to test the effects of the reversion mutation together with the original engineered mutation on 2B/3 cleavage. Cleavage activity of the NS2B–$NS3_{181}$ polyproteins was assayed both in the presence and absence of microsomal membranes, to evaluate more accurately the effects of the mutations on protease function, since differences are observed in the efficiency of processing of the NS2B–$NS3_{181}$ polyprotein under these two conditions (Chambers *et al.*, 1990b). Reactions also were run for intervals of 20, 45 and 90 min, as we found that samples from a single time point (e.g. 60 min) gave differences from one experiment to another, and the time course experiments were better for accurately characterizing the processing.

Fig. 3(a), panel (i) shows that the parental NS2B–$NS3_{181}$ polyprotein exhibited very efficient cleavage, based on the production of its NS2B and $NS3_{181}$ cleavage products. This process was mildly inhibited in the presence of microsomal membranes [panel (ii)]. The NS2B–$NS3_{181}$ polyprotein containing the 2·3·2 mutation exhibited a cleavage efficiency in the absence of membranes that closely resembled the parental protease [panel (i)]. In contrast, the 2·3R polyprotein, containing the revertant mutation at position 45 together with the original alanine mutations, was inefficiently cleaved at 20 min, and even by 90 min cleavage yielded less products than the parental protease. In the presence of membranes [panel (ii)], cleavage of the NS2B–$NS3_{181}$ polyprotein containing the 2·3 mutation was slightly less efficient than that of the parental protease, whereas the 2·3R polyprotein was cleaved to only a minor extent. Fig. 3(a) [panel (ii)] also shows the results for the 2·4 mutation and its revertant. The 2·4 polyprotein was defective in cleavage in the absence of membranes, and the defect was more severe in the presence of membranes. In contrast, the 2·4R polyprotein exhibited more efficient cleavage under both of these conditions.

Fig. 3(b) shows the results for the 2·5 mutation. In the absence of membranes, the NS2B–$NS3_{181}$ polyprotein containing this mutation was cleaved less efficiently than that of the parent over a 90 min interval [panel (i)], whereas the 2·5R polyprotein appeared to be less defective, since more of the precursor was processed into cleavage products at 90 min. The 2·5 polyprotein was less efficiently cleaved in the presence of membranes than in the absence of membranes [panel (ii)]. In contrast, the 2·5R polyprotein underwent slightly more efficient cleavage than 2·5, both in the presence and absence of membranes.

Fig. 3(c), panel (i), shows that the NS2B–$NS3_{181}$ polyprotein containing the 2·18 mutation had no apparent cleavage defect in the absence of membranes, whereas the

Table 2. Classification of revertant viruses

Mutant	Temp. isolated (°C)	Revertant plaque size	Engineered mutation(s)	Revertant mutation(s)	Nucleotide substitutions*
2·3·1	37	Intermediate	$AGRVD_{45–49}$–AGAVA	NS2B A_{47}–E	GGC to GAG
2·3·2	37	Parental	$AGRVD_{45–49}$–AGAVA	NS2B A_{45}–S	GCT to TCT
2·3·3	32	Intermediate	$AGRVD_{45–49}$–AGAVA	NS2B A_{49}–S	GCT to TCT
2·4	37	Intermediate	$ELKK_{52–55}$–ALAK	NS2B A_{54}–V	GCG to GTG
2·5	37	Parental	$ELKK_{52–55}$–ELAK	NS3 R_{62}–W	AGG to TGG
2·18	37	Parental	$LFHVR_{122–126}$–LFAVA	NS2B L_{122}–R	CTG to CGG
3·61	37	Parental	$LEDG_{20–23}$–LADG	NS3 A_{21}–E	GCG to GAG
3·62	37	Parental	$LEDG_{20–23}$–LEAG	NS3 A_{22}–D	GCC to GAC

*Sequence of the original alanine mutation (2·3·1, 2·3·3, 2·4, 3·61, 3·62) or parental residue (2·3·2, 2·5, 2·18, underlined) and the amino acid substitution detected in the revertant viruses.

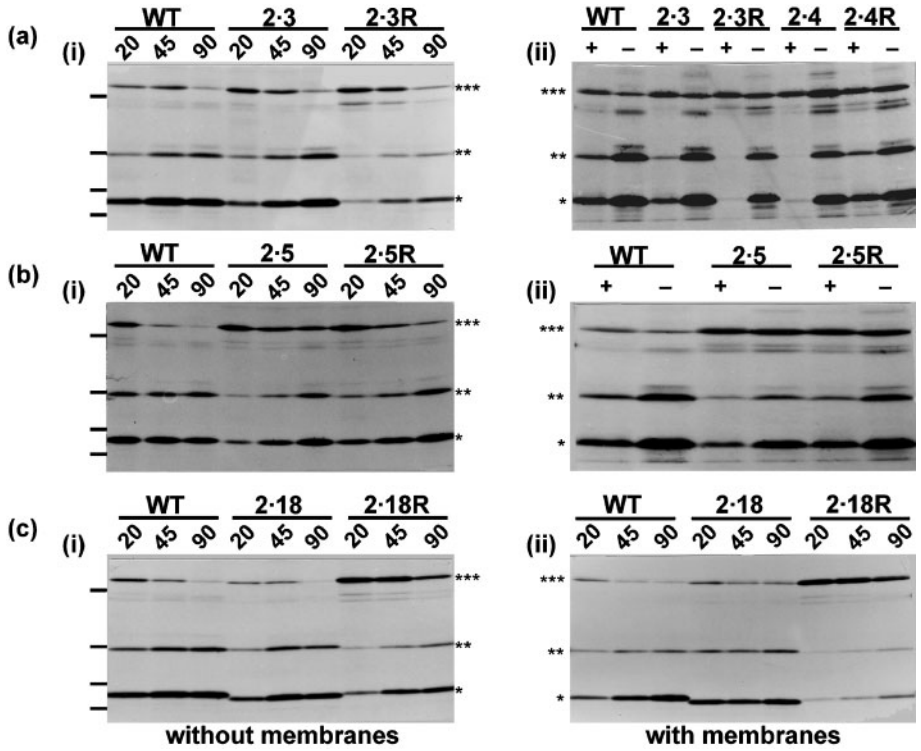

Fig. 3. Cell-free translation of mutant and revertant proteases. pET/BS-NS2B–NS3$_{181}$ plasmids encoding either the original mutant NS2B proteins or NS2B proteins recovered from revertant viruses were used to programme, coupled transcription/translation reactions and the products were immunoprecipitated and analysed by SDS-PAGE, as described in Methods. (a) Mutant 2·3 and 2·3R (mutation plus reversion). Panel (i) indicates time-course in the absence of membranes. Panel (ii) indicates 90 min reactions in the presence or absence of membranes, which includes results for the 2·4 and 2·4R mutations. (b) Mutant 2·5 and 2·5R. Panels are as described for mutant 2·3 (a). (c) Mutant 2·18 and 2·18R. Panel (i) indicates time-course in the absence of membranes. Panel (ii) indicates time-course in the presence of membranes. MW (kDa) are indicated by bars on the left margins, in decreasing order as follows 30, 21·5, 14·3, 12·5. Asterisks indicate polyproteins and cleavage products as follows: ***, NS2B–NS3$_{181}$; ** NS3$_{181}$; *, NS2B.

2·18R polyprotein was markedly impaired. In the presence of membranes, [panel (ii)], the 2·18 polyprotein was only minimally impaired compared to the parent, whereas the 2·18R polyprotein was markedly impaired in cleavage.

Overall, these results indicate that the second-site mutations associated with mutants 2·3, 2·4, 2·5 and 2·18 cause variable effects on the cleavage efficiency of NS2B–NS3$_{181}$ polyproteins. Some (2·4R and 2·5R) improved the cleavage defects caused by the original mutations, whereas others, such as 2·3R and 2·18R, caused deleterious effects.

Effects of reversion mutations on sig2A–5$_{356}$ polyprotein processing

To investigate the effects of reversion mutations on protease-mediated cleavages at other sites in the non-structural polyprotein, pET/BS(+)-sig2A–5$_{356}$ plasmids, encoding both the reversion mutation and the original charged-to-alanine mutation, were constructed and tested for processing of the non-structural polyprotein. Expression of this polyprotein in cells infected with vaccinia virus vTF7-3 allows monitoring of processing events which generate the NS3, NS4A, NS4B and NS5 proteins, and is a surrogate system for analysis of polyprotein processing in virus-infected cells (Chambers *et al.*, 1991). However, the long intervals required for efficient radiolabelling of viral proteins is not amenable to detailed pulse-chase experiments that would allow precise identification of the processing defects caused by mutations. In these experiments, NS4A is not observed (no antiserum is available), and NS5 is not routinely analysed (the antisera react very weakly with the truncated NS5 protein encoded by the plasmid). Only selected mutations that caused small plaques were tested in these experiments. Mutant 2·18 was tested because it had no effect on 2B/3 cleavage and its revertant mutation was very impaired in cleavage of the NS2B–NS3$_{181}$ polyprotein (Fig. 3c). Mutant 3·15 was tested because it exhibited no significant defect in cleavage of the NS2B–NS3$_{181}$ polyprotein. Cleavage of sig2A–5$_{356}$ polyproteins containing the 2·3 or the 2·5 mutations were also studied, but defects of only a minor nature were observed (data not shown).

Fig. 4(a), shows that the 2·18 mutation caused no change in the production of the NS2B protein compared to the parental polyprotein. There was a slight decrease in the

production of NS3 and NS3–4A related proteins (Fig. 4b), and the production of the mature form of NS4B was greatly decreased (Fig. 4c). In contrast, processing of the 2·18R polyprotein containing the 2·18 mutation together with its reversion mutation, yielded levels of NS2B, NS3–4A and NS4B proteins that were similar to those of the parental polyprotein. These data suggest that the 2·18 mutation causes a defect in processing of the NS3-4A and NS4AB-5 regions, which was compensated by the 2·18R mutation.

Fig. 4 also shows that the sig2A–5_{356} polyprotein containing the 3·15 mutation caused a decrease in the production of the NS2B protein associated with an increase in the level of 2A-2B (Fig. 4a). The NS3 protein was greatly reduced (Fig. 4b), but production of NS4B was unaltered (Fig. 4c). These data suggest a deleterious effect of the 3·15 mutation on cleavage at the 2A/2B and 3/4A cleavage sites. No revertant was available for mutant 3·15 to further test this observation. Because differences can occur in this cellular expression system due to variable transfection efficiencies, we repeated these experiments several times using both SW-13 and BHK-21 cells, with consistent results being obtained from one experiment to the next.

Plaque sizes of engineered revertant viruses

Experiments were also conducted to determine whether the second-site mutations that were associated with plaque reversion could increase the plaque size of the small plaque-mutant viruses from which they were originally derived. YF viruses were engineered to contain a portion of the NS2B–$NS3_{181}$ region encompassing the original charged-to-alanine mutation and the associated reversion mutation. This allowed direct testing of the effects of these mutations in the YF5·2iv genetic background, in the absence of mutations outside of the NS2B–$NS3_{181}$ region that might have accumulated during isolation of the original mutants. If an increase of plaque size could be demonstrated in such cases, this would suggest that the reversion mutations within the NS2B–$NS3_{181}$ region contributed compensatory effects during replication of the original mutant virus. For the original 2·5 mutant, the plaque size was 39 % of parental size (Table 1). The plaque size of the virus containing the 2·5 mutation together with the substitution of tryptophan for histidine at NS3 position 62 was 85 % of parental size. For the original 2·18 mutant, the plaque size was 22 % of parental size (Table 1). Virus containing the 2·18 mutation together with the substitution of histidine for leucine at NS2B position 122 gave a plaque size of 70 % of the parental size. These results are consistent with a compensatory effect of the 2·5R and 2·18R mutations on the defect in virus plaque-formation associated with the 2·5 and 2·18 mutations, respectively.

DISCUSSION

In a previous study, we characterized the effects of alanine scanning mutagenesis on cell-free cleavage activity of the NS2B–$NS3_{181}$ protease, to identify charged residues involved in its formation and function (Droll *et al.*, 2000). A few such mutations caused major disruption of cleavage activity, but many others exhibited less severe or even subtle defects on cleavage. We therefore investigated the effects of these mutations on recovery of YF virus infectivity, to attempt to establish correlations between protease cleavage

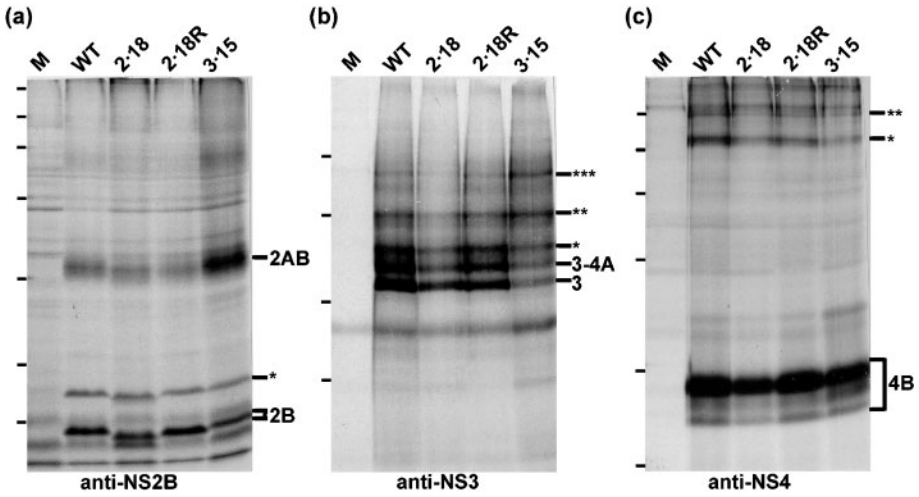

Fig. 4. Transient cellular expression of sig2A–5_{356} polyproteins. (a) Immunoprecipitation with antisera to the YF NS2B protein. (b) Immunuprecipitation with antisera to YF NS3. (c) Immunoprecipitation with antisera to the YF NS4B protein. Mock (M) indicates cells infected with vTF7-3 but treated with lipid in the absence of DNA. 2·18 indicates the polyprotein containing the 2·18 mutation alone; 2·18R indicates polyprotein containing 2·18 and its second-site mutation; 3·15 indicates polyprotein containing the 3·15 mutation. Asterisks indicate positions of putative polyproteins as follows: *, $NS2A^{\alpha}$ (a); ***, NS3–4-5_{356}; **, NS3–4AB; *, NS2–3-4A (b) and **, NS3–4-5_{356}; *, NS3–4AB (c). MW (kDa) are indicated at the left margins of the figures in descending order as follows: (a) and (c): 220, 97·4, 66, 46, 30, 21·5, 14·3 [not shown in part (c)] kDa; (b) 220, 97·4, 66, 46 kDa.

defects and virus production. A range of effects were observed on plaque formation, viral growth efficiency in cell culture and polyprotein processing. In general, deleterious effects of mutations on polyprotein cleavages were related to impaired growth and plaque formation of the corresponding viruses. However, some mutations that essentially caused no defect in 2B/3 cleavage were lethal for virus replication (mutants 2·2, 2·10, 3·21 and 3·25), whereas others showed essentially a parental or reduced level of 2B/3 cleavage but had defects in processing at other cleavage sites in the non-structural polyprotein (2·3, 2·18, 3·15). In the case of mutants 2·4, 2·5 and 2·18, the defects in cleavage activity caused by these mutations at the 2B/3 or other cleavage sites could be partially compensated by second-site mutations in either NS2B or NS3.

In the case of the 2·3 mutation, which targeted a charge cluster at the proximal end of the conserved domain of NS2B, a defect in cleavage of the NS2B–$NS3_{181}$ polyprotein in the presence of membranes was observed, and subtle defects in processing of other non-structural cleavage sites were observed. Several reversion mutations were mapped to the same site or a site adjacent to the original mutation, involving charged (glutamic acid) or uncharged polar (serine) amino acid substitutions. These findings suggest that the interaction of a NS2B with NS3 depends on a charge cluster at positions 47 and 49 of NS2B, presumably through effects on complex formation, and consistent with previous studies (Chambers *et al.*, 1993). In the absence of the charge interactions, the serine substitutions at positions 45 and 49 might promote binding of NS2B to NS3 as a result of hydrogen bond interactions of their hydroxyl groups with residues in the binding cleft on NS3 (see below). Cell-free cleavage of the NS2B–$NS3_{181}$ polyprotein revealed that the 2·3R mutation was defective in cleavage compared with 2·3, and thus 2B/3 cleavage efficiency did not correlate with plaque size for the 2·3 mutant and its revertants. However, this assay may not accurately reflect processing of this site in the context of a full-length non-structural polyprotein, where interactions of multiple viral and host proteins could result in different effects at the 2B/3 and other cleavage sites when comparing mutant and revertant proteases.

The 2·18 mutation was associated with defects in the production of NS3–4A polyproteins and NS4B from the sig2A–5_{356} polyprotein. This observation suggests that the interaction of the protease complex with the polyprotein substrate during the cleavages at the 3/4A, and 4B/5 cleavage sites may be impaired. A second-site mutation associated with the 2·18 mutation partially restored the polyprotein processing defects, as well as led to an increase in the plaque forming capacity of the corresponding mutant virus. The proximity of the reversions to the original mutation suggests that its effects may be mediated through preservation of a charge cluster involved in local structural integrity or membrane association of NS2B. However, the observation that cleavages affecting the production of NS3–4A and NS4B were primarily affected suggests that the mutations and reversions may also cause effects on substrate binding in the downstream region of the polyprotein.

Introduction of the 2·18R mutation together with the original 2·18 mutation into the YF5·2iv infectious clone yielded virus with a plaque size larger than that of the 2·18 mutant itself. This suggests that the improvement in polyprotein processing associated with the revertant substitution contributes to more efficient virus replication. Although cleavage efficiency of the 2·18R mutation at the 2B/3 cleavage site (Fig. 3c) did not correlate with the ability of this mutation to affect plaque size, the cell-free cleavage assay of the NS2B–$NS3_{181}$ polyprotein may not accurately reflect the processing of this site in the context of a full-length non-structural polyprotein, as discussed for the 2·3 and 2·3R mutations. In support of this, results shown in Fig. 4 indicate that the 2·18R mutation does not in fact compromise production of NS2B, as suggested by the cell-free cleavage assay (Fig. 3c).

For the 3·15 mutation, the cleavage defects included a decreased cleavage of the NS2AB protein and reduced production of NS3 and NS3–4A-related proteins. These results are consistent with a deleterious effect of this mutation on the interaction of the NS2B–$NS3_{181}$ complex with the 2A/2B, 3/4A, and 4A/4B cleavage sites, more than the 2B/3 or 4B/5 sites. This may result from a specific interaction of the three charged residues targeted by the mutation with the substrate contacts in the 3/4A and 2A/2B regions, which differ from interactions at the 2B/3 and 4B/5 cleavage sites. Since no second-site mutation was available for the 3·15 mutation, no further explanation of its cleavage defect can be given at this time.

The 2·5 mutation was characterized by a reduced level of 2B/3 cleavage efficiency. This mutant had a second-site mutation in a region of the NS3 protease that, based on the 3D structure of dengue-2 protease, has been implicated as part of the binding site for its NS2B cofactor (Matusan *et al.*, 2001). In that study, residues $KRIE_{63–66}$ in the dengue-2 NS3 protease were predicted to be solvent-exposed and likely to make contact with the N-terminal portion of the conserved domain of NS2B, which corresponds to the location of mutation 2·5. To gain insight into the relationship between the 2·5 mutation and its NS3 reversion mutation, we derived a homology model for the YFV NS3 protease and analysed the effects of a tryptophan substitution at position 62 (Fig. 5). Using predictions for the dengue-2 virus structure as a guide (Matusan *et al.*, 2001), tryptophan is predicted to interact with the alanine substitution at position 55 in NS2B. In support of this, comparison of sequence alignments of 12 flavivirus sequences showed that only Langat, tick-borne encephalitis and Powassan viruses have non-polar residues at residue 62 in NS3 (YF numbering), and a hydrophobic residue (tryptophan) at position 55 of the YFV NS2B (data not shown). In contrast, all other flaviviruses have hydrophilic residues, (either arginine or lysine) at position 55. Only in YFV is an arginine in NS3 paired with a lysine in NS2B. Although both of

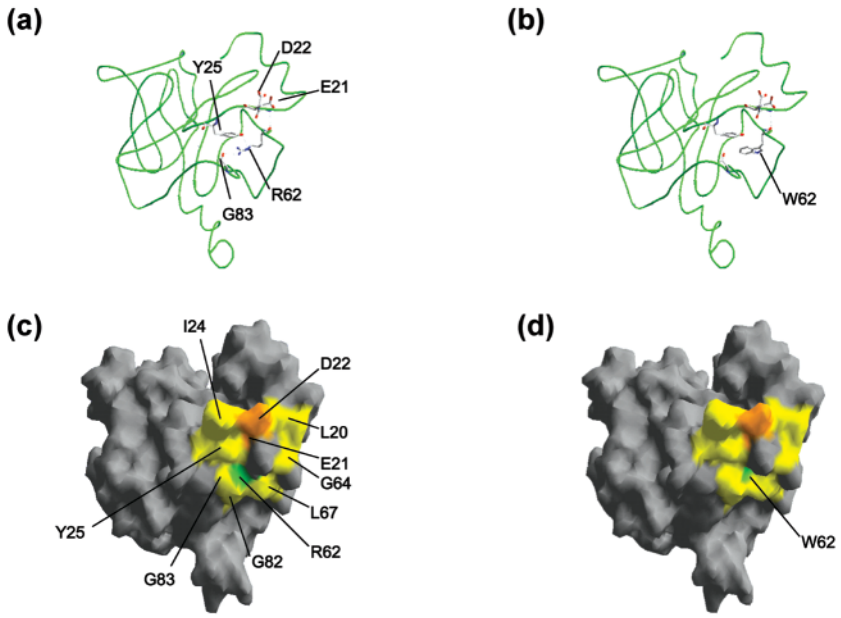

Fig. 5. Homology model of the YFV NS3 protease based on the dengue-2 protease. (a) and (b) depict the ribbon structures of the parental and revertant YFV proteases, with the position of residue 62 shown. (c) and (d) depict the corresponding space-filling structures for the same proteases. The positions of parental arginine and the tryptophan reversion at residue 62 are indicated by green shading. Yellow shading indicates the hydrophobic surface formed by leucine residues at positions 20 and 67, glycine at positions 64, 82 and 83, and isoleucine at position 24. The orange residues indicate glutamic acid and aspartic acid at positions 21 and 22, which have been previously implicated in the interaction of NS3 with NS2B during formation of the protease complex (Droll *et al.*, 2000).

these residues carry positive charges, a van der Waals-type interaction may occur between them. Replacement of lysine by alanine at NS2B position 55 would create some empty space (four methylene groups) and substitution of the more bulky tryptophan for arginine at NS3 position 62 would fill the space and retain hydrogen bonding ability, through the side chain of tryptophan. Our hypothesis is that lysine, leucine and glutamic acid at positions 55, 56 and 58 of NS2B bind in a pocket on NS3 lined by surrounding hydrophobic and non-polar residues (leucine at positions 20 and 67, isoleucine at position 24, glycine at positions 82 and 83). An interaction of tryptophan at NS3 position 62 with alanine at NS2B position 55 may be stabilized due to effects of this hydrophobic contact region. According to this model, the 2·5R mutation improves binding interactions in the hydrophobic pocket, leading to improved protease cleavage activity and contributing to more efficient virus replication.

In addition to the direct effects of the mutants and revertants studied in these experiments, it is possible that other factors operate to cause a reduction in plaque size of the corresponding viruses. These might include effects of the mutations on RNA secondary structure, protein translation and/or viral packaging. In this regard, mutations in the NS2A protein have been shown to cause defects in the assembly of the YFV, although the mechanism is unknown (Kummerer & Rice *et al.*, 2002). Although we do not have direct evidence to rule out these possibilities, it seems less likely that the reversion mutations observed here would mediate such effects, as compared with direct effects on the cleavage activity of the NS2B–NS3 protease complex.

The observation that no second-site revertants could be obtained from mutations in the NS3 region, together with the fact that most lethal alanine substitutions occurred in NS3, may indicate a strong selection against mutations which perturb the conserved structure of this domain, and a low tolerance for secondary mutations, which might otherwise provide compensatory effects. In contrast to NS3, mutations may be more readily tolerated in NS2B, which may undergo a dynamic interaction with the loosely structured amino terminus of NS3, as appears to be the case for the NS3 protease of hepatitis C virus (Satoh *et al.*, 1995; Love *et al.*, 1998).

In conclusion, our results suggest the existence of protein–protein interactions among the NS2B–NS3 protease and non-structural proteins that affect folding of the polyprotein and access of the protease to the non-structural cleavage sites. Further experiments, such as *trans* cleavage assays of mutant and revertant NS2B–NS3 proteases and substrate polyproteins, as well as mutagenesis of regions surrounding the cleavage sites, which are inefficiently cleaved in the presence of the protease mutations, may be of interest. These should reveal more details of the molecular determinants governing normal processing of the YFV non-structural polyprotein.

ACKNOWLEDGEMENTS

This work was supported by grants from the NIAID (AI-38574) and the CDC (CI00094).

REFERENCES

Amberg, S. M., Nestorowicz, A., McCourt, D. W. & Rice, C. M. (1994). NS2B-3 proteinase-mediated processing in the yellow fever virus structural region: in vitro and in vivo studies. *J Virol* **68**, 3794–3802.

Arias, C. F., Preugschat, F. & Strauss, J. H. (1993). Dengue 2 virus NS2B and NS3 form a stable complex that can cleave NS3 within the helicase domain. *Virology* **193**, 888–899.

Bazan, J. F. & Fletterick, R. J. (1989). Detection of a trypsin-like serine protease domain in flaviviruses and pestiviruses. *Virology* **171**, 637–639.

Brinkworth, R. I., Fairlie, D. P., Leung, D. & Young, P. R. (1999). Homology model of the dengue 2 virus NS3 protease: putative interactions with both substrate and NS2B cofactor. *J Gen Virol* **80**, 1167–1177.

Butkiewicz, N. J., Wendel, M., Zhang, R. & 10 other authors (1996). Enhancement of hepatitis C virus NS3 proteinase activity by association with NS4A-specific synthetic peptides: identification of sequence and critical residues of NS4A for the cofactor activity. *Virology* **225**, 328–338.

Cahour, A., Falgout, B. & Lai, C.-J. (1992). Cleavage of the dengue virus polyprotein at the NS3/NS4A and NS4B/NS5 junctions is mediated by viral protease NS2B-NS3, whereas NS4A/NS4B may be processed by a cellular protease. *J Virol* **66**, 1535–1542.

Chambers, T. J., McCourt, D. W. & Rice, C. M. (1990a). Production of yellow fever virus proteins in infected cells: identification of discrete polyprotein species and analysis of cleavage kinetics using region-specific polyclonal antisera. *Virology* **177**, 159–174.

Chambers, T. J., Weir, R. C., Grakoui, A., McCourt, D. W., Bazan, J. F., Fletterick, R. J. & Rice, C. M. (1990b). Evidence that the N-terminal domain of nonstructural protein NS3 from yellow fever virus is a serine protease responsible for site-specific cleavages in the viral polyprotein. *Proc Natl Acad Sci U S A* **87**, 8898–8902.

Chambers, T. J., Grakoui, A. & Rice, C. M. (1991). Processing of the yellow fever virus nonstructural polyprotein: a catalytically active NS3 proteinase domain and NS2B are required for cleavages at dibasic sites. *J Virol* **65**, 6042–6050.

Chambers, T. J., Nestorowicz, A., Amberg, S. M. & Rice, C. M. (1993). Mutagenesis of the yellow fever virus NS2B protein: effects on proteolytic processing, NS2B-NS3 complex formation and viral replication. *J Virol* **67**, 6797–6807.

Chambers, T. J., Nestorowicz, A. & Rice, C. M. (1995). Mutagenesis of the yellow fever virus NS2B/3 cleavage site: determinants of cleavage site specificity and effects on polyprotein processing and viral replication. *J Virol* **69**, 1600–1605.

Droll, D. A., Krishna-Murthy, H. M. & Chambers, T. J. (2000). Yellow fever virus NS2B-NS3 protease: charged-to-alanine mutagenesis and deletion analysis define regions important for protease complex formation and function. *Virology* **275**, 335–347.

Falgout, B. & Markoff, L. (1995). Evidence that flavivirus NS1-NS2A cleavage is mediated by a membrane-bound host protease in the endoplasmic reticulum. *J Virol* **69**, 7232–7243.

Falgout, B., Pethel, M., Zhang, Y. M. & Lai, C.-J. (1991). Both nonstructural proteins NS2B and NS3 are required for the proteolytic processing of dengue virus nonstructural proteins. *J Virol* **65**, 2467–2475.

Falgout, B., Miller, R. H. & Lai, C.-J. (1993). Deletion analysis of dengue virus type 4 nonstructural protein NS2B: identification of a domain required for NS2B-NS3 proteinase activity. *J Virol* **67**, 2034–2042.

Gorbalenya, A. E., Donchenko, A. P., Koonin, E. V. & Blinov, V. M. (1989). N-terminal domains of putative helicases of flavi- and pestiviruses may be serine proteases. *Nucleic Acids Res* **17**, 3889–3897.

Kummerer, B. M. & Rice, C. M. (2002). Mutations in the yellow fever virus nonstructural protein NS2A selectively block production of infectious particles. *J Virol* **76**, 4773–4784.

Lin, C., Amberg, S. M., Chambers, T. J. & Rice, C. M. (1993a). Cleavage at a novel site in the NS4A region by the yellow fever virus NS2B-3 proteinase is a prerequisite for processing at the downstream 4A/4B signalase site. *J Virol* **67**, 2327–2335.

Lin, C., Chambers, T. J. & Rice, C. M. (1993b). Mutagenesis of conserved residues at the yellow fever 3/4A and 4B/5 dibasic cleavage sites: effects on cleavage efficiency and polyprotein processing. *Virology* **192**, 596–604.

Lin, C., Thomson, J. A. & Rice, C. M. (1995). A central region in the hepatitis C virus NS4A protein allows formation of an active NS3-NS4A serine proteinase complex in vivo and in vitro. *J Virol* **69**, 4373–4380.

Lindenbach, B. D. & Rice, C. M. (2001). *Flaviviridae.* In *Fields Virology*, 3rd edn, pp. 991–1041. Edited by D. M. Knipe, P. M. Howley, D. E. Griffin, R. A. Lamb, M. A. Martin, B. Roizman & S. E. Straus. Philadelphia: Lippincott.

Lobigs, M. (1992). Proteolytic processing of a Murray Valley encephalitis virus non-structural polyprotein segment containing the viral proteinase: accumulation of a NS3-4A precursor which requires mature NS3 for efficient processing. *J Gen Virol* **73**, 2305–2312.

Lobigs, M. (1993). Flavivirus premembrane protein cleavage and spike heterodimer secretion require the function of the viral proteinase NS3. *Proc Natl Acad Sci U S A* **90**, 6218–6222.

Love, R. A., Parge, H. E., Wickersham, J. A. & 7 other authors (1998). The conformation of hepatitis C virus NS3 proteinase with and without NS4A: a structural basis for the activation of the enzyme by its cofactor. *Clin Diagn Virol* **19**, 151–156.

Matusan, A. E., Pryor, M. J., Davidson, A. D. & Wright, P. J. (2001). Mutagenesis of the Dengue virus type 2 NS3 protein within and outside helicase motifs: effects on enzyme activity and virus replication. *J Virol* **75**, 9633–9643.

Murthy, H. K., Clum, S. & Padmanabhan, R. (1999). Dengue virus NS3 serine protease. Crystal structure and insights into interaction of the active site with substrates by molecular modeling and structural analysis of mutational effects. *J Biol Chem* **274**, 5573–5580.

Nestorowicz, A., Chambers, T. J. & Rice, C. M. (1994). Mutagenesis of the yellow fever virus NS2A/2B cleavage site: effects on proteolytic processing, viral replication and evidence for alternative processing of the NS2A protein. *Virology* **199**, 114–123.

Preugschat, F. & Strauss, J. H. (1991). Processing of nonstructural proteins NS4A and NS4B of dengue 2 virus in vitro and in vivo. *Virology* **185**, 689–697.

Preugschat, F., Yao, C.-W. & Strauss, J. H. (1990). In vitro processing of dengue 2 nonstructural proteins NS2A, NS2B, and NS3. *J Virol* **64**, 4364–4374.

Rice, C. M., Grakoui, A., Galler, R. & Chambers, T. J. (1989). Transcription of infectious yellow fever virus RNA from full-length cDNA templates produced by *in vitro* ligation. *New Biol* **1**, 285–296.

Satoh, S., Tanji, Y., Hijikata, M., Kimura, K. & Shimotohno, K. (1995). The N-terminal region of hepatitis C virus nonstructural protein 3 (NS3), is essential for stable complex formation with NS4A. *J Virol* **69**, 4255–4260.

Studier, F. W., Rosenberg, A. H., Dunn, J. J. & Dubendorff, J. W. (1990). Use of T7 RNA polymerase to direct expression of cloned genes. *Methods Enzymol* **185**, 60–89.

Teo, K. F. & Wright, P. J. (1997). Internal proteolysis of the NS3 protein specified by dengue virus 2. *J Gen Virol* **78**, 337–341.

Wengler, G., Czaya, G., Farber, P. M. & Hegemann, J. H. (1991). In vitro synthesis of West Nile virus proteins indicates that the amino terminal segment of the NS3 protein contains the active centre of the protease which cleaves the viral polyprotein after multiple basic amino acids. *J Gen Virol* **72**, 851–858.

Yamshchikov, V. F. & Compans, R. W. (1994). Processing of the intracellular form of the West Nile virus capsid protein by the viral NS2B-NS3 protease: an in vitro study. *J Virol* **68**, 5765–5771.

Yamshchikov, V. F. & Compans, R. W. (1995). Formation of the flavivirus envelope: role of the viral NS2B-NS3 protease. *J Virol* **69**, 1995–2003.

Yusof, R., Clum, S., Wetzel, M., Murthy, K. H. M. & Padmanabhan, R. (2000). Purified NS2B/NS3 serine protease of dengue virus type 2 exhibits cofactor NS2B dependence for cleavage of substrates with dibasic amino acids *in vitro*. *J Biol Chem* **275**, 9963–9969.

Zhang, L., Mohan, P. M. & Padmanabhan, R. (1992). Processing and localization of Dengue virus type 2 polyprotein precursor NS3-NS4A-NS4B-NS5. *J Virol* **66**, 7549–7554.